

Discrepancies between experiment and theory in the superconducting proximity effect

M. Zhang, G. Tateishi, and G. Bergmann

Department of Physics, University of Southern California, Los Angeles, California 90089-0484, USA

(Received 24 February 2006; revised manuscript received 4 May 2006; published 12 July 2006)

The superconducting proximity effect is investigated for SN double layers in a regime where the resulting transition temperature T_c does not depend on the mean free paths of the films and, within limits, not on the transparency of the interface. The experimental results for T_c are compared with a numerical evaluation which was recently developed in our group. The results for the SN double layers can be divided into three groups. (i) When $N=\text{Cu, Ag, Au, Mg}$ a disagreement between experiment and theory by a factor of the order of 2.5 is observed. (ii) When $N=\text{Cd, Zn, Al}$ the disagreement between experiment and theory is reduced to a factor of about 1.5. (iii) When $N=\text{In, Sn}$ a reasonably good agreement between experiment and theory is observed.

DOI: [10.1103/PhysRevB.74.014506](https://doi.org/10.1103/PhysRevB.74.014506)

PACS number(s): 74.45.+c, 73.40.Jn, 74.78.Fk

I. INTRODUCTION

The properties of a superconducting film or thin wire S are modified when they are in contact with a normal metal N . This phenomenon was first observed in the pioneering experiments by Meissner¹ who explored the properties of superconducting wires covered with normal metals. It is generally called the “superconducting proximity effect” (SPE). It was intensively studied in the 1960’s.^{2–8} During the last decade it has experienced a renewed interest theoretically,^{9–22} as well as experimentally.^{17,19,23–30} Recently the SPE has been extended to SN multilayers.^{31–33}

A few years ago, our group²⁹ investigated the proximity effect between Pb and several alkali metals. For a better analysis of these measurements we developed a quantitative numerical method for the calculation of the transition temperature of an SN double layer.³⁴ Our numerical results show that, when a superconductor S is covered with a normal metal N , that the initial slope dT_c/dd_n is independent of the mean free paths of the two metals and the transmission of the interface (if the transmission is not dramatically changed). If one defines a normalized initial slope $S_{sn} = \frac{d_s}{T_s} \left| \frac{dT_c}{dd_n} \right|$ then S_{sn} is independent of the thickness d_s of the superconductor up to relatively large values of d_s .

When we compared our experimental initial slope $\left. \frac{dT_c}{dd_n} \right|_{d_n=0}$ with our numerical calculation we observed that the experimental results were considerably smaller than the theoretical predictions. Surprised by the discrepancy we searched the literature and found early experiments from the 1960s, particularly by Hilsch^{2,3} and Minigerode,⁷ from which the normalized initial slope can be derived. These measurements showed a similar disagreement in the initial slope with the theory (see Ref. 34).

Since we were rather amazed by the discrepancy between our experiments and theory in the SPE and also by the fact that this discrepancy had not been detected previously, we decided to reinvestigate the SPE. In this paper we investigate the SPE in the range where a minimum of experimental parameters is needed to perform a quantitative comparison with the theory. We focus on the normalized initial slope S_{sn} of SN double layers and the transition temperature of very thin NS double layers in the thin film regime.

In the present investigation we use only simple (s,p) metals for the superconductors and normal conductors. The su-

perconducting properties of an (s,p) metal can be reasonably well described by a single attractive electron-electron interaction V_{BCS} and a single density of states. In contrast a transition metal has not only an (s,p) band but also several d bands. Each band has its individual BCS interaction and density of states. The large number of (not well known) parameters makes a numerical treatment of the SPE in transition metals difficult and rather inconclusive. Furthermore, when a transition metal film is in contact with an (s,p) metal film its d electrons have first to be scattered into its (s,p) band before they can cross the interface. This takes a finite time τ_{sd} . The superconducting behavior of the double layer depends strongly on the relative size of $1/\tau_{sd}$ and $1/\tau_{T_c}$ [where $\tau_{T_c} = \hbar / (2\pi k_B T_c)$ is characteristic time of a superconductor at the temperature T_c]. The magnitude of $1/\tau_{sd}$ depends strongly on the mean free path in the transition metal film and is difficult to measure. Furthermore the d density of states can strongly depend on the disorder, i.e., the mean free path of the transition metal. For this reason we use only simple (s,p) metal films in this investigation. In first approximation a finite mean free path does not change their properties dramatically.

II. EXPERIMENT AND RESULTS

For the investigation of the SPE it is very important that the metal films are homogeneous and smooth. In particular the formation of islands and a diffusion between films at the interface has to be excluded. For this reason we use the method of quenched condensation onto a substrate of helium temperature. Our initial substrate is a crystalline quartz plate. In a zero evaporation step the quartz plate is covered with ten atomic layer of amorphous insulating Sb. The Sb film acts as a fresh substrate and insures that the following quench condensed films are flat and homogeneous. The (s,p) metals which are condensed on top of the amorphous Sb become already conducting at a thickness between two and four atomic layers. Generally we increase the thickness of the first metal film at least to four times this thickness of first conductance.

When a second metal is quench condensed onto the first metal it does not diffuse into the first one. (Alkali metals which are not used in this investigation may be an excep-

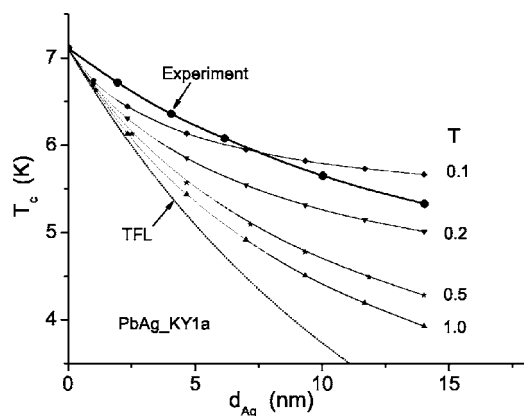


FIG. 1. T_c versus d_{Ag} for a PbAg double layer. The big full circles are the experimental results. The numbers below T give the reduction of transmission through the interface.

tion.) The two metals form an interface with atomic roughness but no mixing. This is extremely important because double or multi layers which are prepared at room temperature are generally interdiffused and form an alloy several atomic layers thick. Such an alloy can be a superconductor with a very different transition temperature spoiling the investigation.

We use thermal evaporation to condense the thin films onto the substrate at liquid helium temperature. To obtain clean films all the evaporation sources are surrounded with liquid N_2 and the vacuum in our system is better than 10^{-11} Torr.

In a series of experiments a film of the superconductor Pb is first condensed onto the Sb substrate. Afterwards the Pb is covered in several step with an increasing thickness of the normal metal Ag. The thickness of the films is measured with a quartz oscillator. The accuracy of the thickness measurement is about 15%. After each evaporation the superconducting transition curve of the double layer is measured. Figure 1 shows a plot of T_c versus the Ag thickness d_{Ag} on top of a 25.1-nm-thick Pb film. The big full circles are the experimental points (which are obtained from a single experiment). This plot yields graphically the initial slope $dT_c/dd_n|_{d_n=0}$ and the normalized initial slope S_{sn}

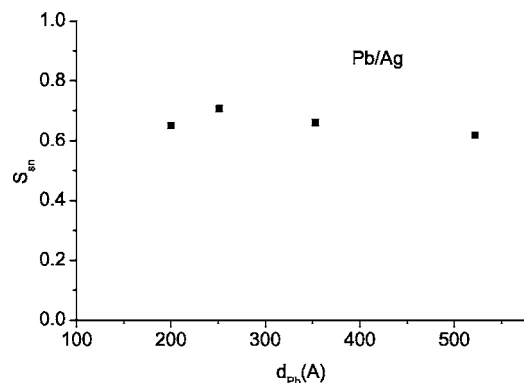


FIG. 2. The normalized initial slope S_{sn} for the Pb/Ag double layers as a function of the Pb thickness.

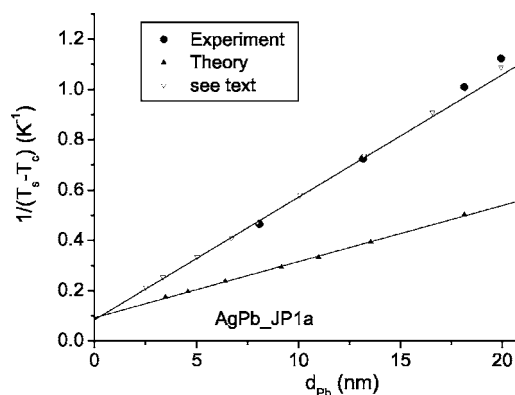


FIG. 3. The inverse T_c reduction $1/(T_s - T_c)$ versus the Pb thickness d_{pb} for double layers of Ag/Pb. The big circles give the experimental points. The other symbols are explained in the discussion.

$$S_{sn} = \frac{d_s}{T_s} \left| \frac{dT_c(d_n=0)}{dd_n} \right|, \quad (1)$$

where $d_{pb}=d_s$ is the thickness of the Pb films and $T_s = 7.2$ K is the transition temperature for Pb. The other curves will be explained in the discussion.

This experiment is repeated for different thicknesses of the superconductor Pb. In Fig. 2 S_{sn} is plotted for different thicknesses d_{pb} of the Pb substrate. It is essentially independent of the Pb thickness. This is in agreement with our numerical results. The value of the normalized initial slope is $S_{PbAg} = 0.66 \pm 0.05$.

In a second set of experiments we investigate the superconducting proximity effect in the thin film regime. For this purpose a thin film of the normal metal (about 3-nm thick) is quench condensed onto the insulating Sb substrate. Then it is covered in a sequence of evaporations with increasing Pb thickness. For the first layer (the normal metal) we use Ag, Au, Cu, Mg. Furthermore we included also as N superconductors with a transition temperatures T_n which lie below the value of T_c for Pb. These metals are Zn, Cd, Al, In, and Sn. Figure 3–6 shows some of the results for Ag/Pb, Mg/Pb, Zn/Pb, and Sn/Pb double layers. In these figures $(T_s - T_c)^{-1}$ is plotted versus the Pb thickness d_{pb} . The big full points are

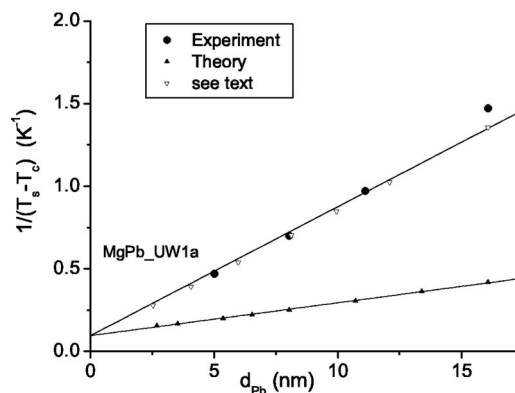


FIG. 4. The inverse T_c reduction $1/(T_s - T_c)$ versus the Pb thickness d_{pb} for double layers of Mg/Pb.

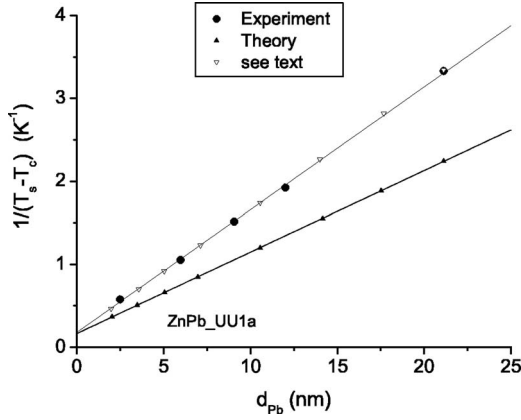


FIG. 5. The inverse T_c reduction $1/(T_s - T_c)$ versus the Pb thickness d_{pb} for double layers of Zn/Pb.

the experimental results. Within the coherence length of the Pb which is about 13 nm (see below) $(T_s - T_c)^{-1}$ of the experimental points is a linear function of d_{pb} . The other symbols will be discussed below.

III. DISCUSSION

When the superconducting proximity effect was first investigated the original goal was to study the length dependence of superconductivity. In a double layer of a normal and a superconductor the gap function Δ depends on z , the position perpendicular to the layers. If the thickness of the superconducting layer surpasses the coherence length then $\Delta(z)$ approaches the equilibrium value (at the free surface of the superconductor) and T_c of the double layer approaches T_s , the transition temperature of the pure superconductor.

The mechanism which determines the gap function $\Delta(z)$ is a complex interplay of the propagation of the pair amplitude (of the Cooper pairs) between the superconducting and normal conducting layers, its exponential decay due to the finite temperature as $\exp(-t/\tau_T)$ (where $1/\tau_T = 2\pi k_B T/\hbar$), and the fresh condensation due to the attractive BCS interaction V_{BCS} . The physics can be treated as a dynamic process between decay and creation of the pair amplitude. At the

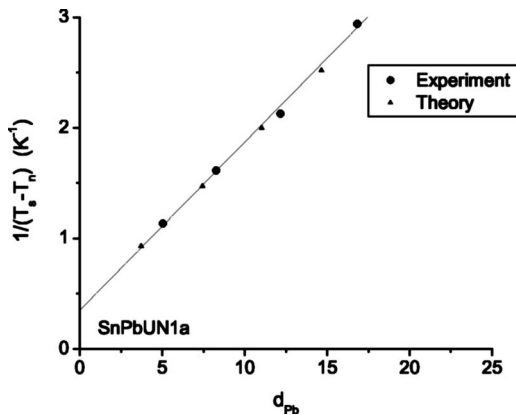


FIG. 6. The inverse T_c reduction $1/(T_s - T_c)$ versus the Pb thickness d_{pb} for double layers of Sn/Pb.

transition temperature decay and creation exactly balance each other. One of the authors recently interpreted the superconducting proximity effect as such dynamic interplay between decay and balance.³⁴ A numerical procedure for the calculation of the transition temperature and the gap function was derived. A number of examples were evaluated. The physical picture behind this approach is briefly reviewed in the Appendix.

A. Thin film regime

The distance which an electron (or a pair amplitude) propagates during the time $\tau_T = \hbar/(2\pi k_B T_s)$ determines a superconducting coherence length ξ . For a pure superconductor it is the ballistically traveled distance ξ_0 , while for a disordered superconductor it is the diffusively traveled distance ξ'_0 , where

$$\xi_0 = v_F \tau_T = \hbar v_F / (2\pi k_B T_s),$$

$$\xi'_0 = \sqrt{D\tau_T} = \sqrt{v_F \tau_T l / 3} = \sqrt{\xi_0 l / 3} = \sqrt{\hbar v_F l / (6\pi k_B T_s)}. \quad (2)$$

Here v_F is the Fermi velocity, $D = v_F l / 3$ is the diffusion constant, l is the mean free path, and T_s is the transition temperature of the pure superconductor S . In the superconductor S we denote both length ξ_0 and ξ'_0 as the pair coherence lengths. The corresponding lengths in N at the same temperature are called thermal coherence lengths.

The spatial dependence of $\Delta(z)$ depends on a different coherence length, often called the Ginzburg-Landau coherence length. In the vicinity of T_s it is given by $\xi_{GL} = \frac{\pi}{2} \xi_0 [(T_s - T)/T_s]^{-1/2}$ and diverges at T_s . In first approximation the gap function varies in the superconductor as $\cos[(z + d_s)/\xi_{GL}]$ and in the normal conductor as $\cosh[(z - d_n)/\xi_{GL}]$ (see, for example, Werthamer³⁵).

When the thicknesses of the superconductor and normal conductor are both much smaller than their Ginzburg-Landau coherence lengths the system is in the thin film limit or Cooper limit. In that case the gap function is essentially constant in each film.

Cooper⁴³ considered the thin film limit first and averaged the BCS interaction over both films as

$$V_{\text{eff}} = \frac{V_s d_s + V_n d_n}{d_s + d_n}.$$

DeGennes³⁶ pointed out that it is the product NV that should be averaged and the weight is proportional to the product of thickness times density of states. When the metal N has vanishing BCS interaction, $V_n = 0$, deGennes obtained for the effective interaction parameter $(NV)_{\text{eff}}$

$$(NV)_{\text{eff}} = (NV)_s \frac{N_s d_s}{N_s d_s + N_n d_n} \quad (3)$$

which yields the implicit condition for the transition temperature T_c

$$\frac{1}{(NV)_{\text{eff}}} = \sum_{n=0}^{n_c} \frac{1}{n + \frac{1}{2}}, \quad (4)$$

where the upper limit of the summation $n_c = \Theta_D / (2\pi T_c)$, determines the transition temperature.

A special case of the thin film limit is the weak coupling limit where $\Theta_D \gg 2\pi T_c$. In this case, which we denote as Cooper limit, the transition temperature of the double layer is given by the BCS-Cooper equation

$$T_c = 1.14 \Theta_D \exp\left(-\frac{1}{(NV)_{\text{eff}}}\right). \quad (5)$$

The resulting normalized initial slope for an S/N double layer is in the Cooper limit

$$S_{Cp} = \frac{d_s}{T_s} \left| \frac{dT_c}{dd_n} \right| = d_s \left| \frac{d[\ln(T_c)]}{dd_n} \right| = \frac{N_n}{N_s} \frac{1}{(NV)_s}. \quad (6)$$

S_{Cp} is proportional to the ratio of the density of states N_n/N_s and inversely proportional to the BCS interaction parameter $(NV)_s$. If one is not in the weak-coupling limit, but still in the thin film limit [using Eq. (4) for the transition temperature] the normalized initial slope is still proportional to N_n/N_s . But $(NV)_s^{-1}$ is replaced by a value which has to be determined numerically.

In the thin film limit (including the Cooper limit) the transition temperature and the normalized initial slope do not depend on the mean free paths or the coherence lengths of the two films.

For the case that both metals S and N are superconducting deGennes derived two equations for the gap functions in the thin film limit. In this case one has a constant gap in each film, Δ_s in S and Δ_n in N . We rederive deGennes' results in the Appendix as a special example of our numerical method.

All our experiments are performed in the thin film regime. For this regime the thin film results are a good approximation. However, since all experimental films have a finite thickness, one has to expect (small) deviations between the predictions of the thin film limit and the full theory (not restricted to the thin film limit). Therefore we always use the full theory for the theoretical predictions. In selected examples we discuss the agreement (deviation) between the thin film limit and the full theory. The full numerical theoretical treatment is discussed in details in Ref. 34 and the essential points are reviewed in the Appendix.

B. Initial slope

The measurement of the initial slope in our PbAg double layers is an experiment in the thin film regime. In Fig. 1 the transition temperature of a PbAg double layer is plotted as a function of the Ag thickness d_{Ag} . In Ref. 34 we calculated the normalized initial slope $S_{sn} = (d_s/T_s) |dT_c/dd_n|$ as a function of the thickness of the superconductor and observed that S_{sn} is essentially constant up to relatively large values of d_s . This means that the thin film regime extends in this case much further than one would naively expect. The physical reason is following. Let us consider different PbAg

double layers with a small constant thickness d_n of the normal conductor. For a given thickness d_s of the superconductor the reduction of the transition temperature is $\Delta T_c = (T_s - T_c) = S_{sn} T_s / d_s$. At this temperature the Ginzburg-Landau coherence length is $\xi_{\text{GL}} = \frac{\pi}{2} \xi_{\text{BCS}} \sqrt{T_s / (T_s - T_c)} = \frac{\pi}{2} \xi_{\text{BCS}} \sqrt{d_s / S_{sn}}$. This means that the relevant coherence length grows with increasing thickness of the superconductor and can by far exceed the pair coherence length. For example the first Ag point in Fig. 1 with $d_{\text{Ag}} \approx 2$ nm has a reduction of $\Delta T_c \approx 0.4$ K. This yields $\xi_{\text{GL}} \approx 7 \xi_0$.

The full big circles in Fig. 1 represent the experimental T_c values. It has an normalized initial slope of $S_{\text{exp}} = 0.66$. The lower curve with the up triangles gives the theoretical prediction using the full theory. It yields for the normalized initial slope the values $S_{\text{theo}} = 1.75$. For a comparison Fig. 1 shows also the thin film limit results for the transition temperature as the dotted curve marked as TFL. Its transition temperatures are calculated with Eq. (4) using the effective interaction parameter of Eq. (3). The TFL curve has the same normalized initial slope of $S_{\text{TFL}} = 1.75$ as the full theory but for larger Ag thicknesses it deviates considerably from the full theory.

Obviously the theory yields a much larger reduction of T_c . As discussed above the input parameters are the thickness d_{pb} , d_{Ag} , the Debye temperature Θ_D of Pb (Θ_D of Ag does not enter the gap equation for Δ_s), the (experimental) density of states N_{pb} , N_{Ag} and the transition temperature of Pb. The interaction parameter $(NV)_{\text{pb}}$ is self-consistently determined from the transition temperature T_{pb} . The density of states are taken from Kittel³⁷ and include the electron-phonon enhancement. The ratio between the experimental and the theoretical slope is 0.38. This is a remarkably large discrepancy between experiment and theory.

Transmission of the interface. A major concern in the study of the SPE is the transmission through the interface between the layers of S and N . The probability to find an electron in film S or N is proportional to the product of thickness and density of state, i.e., $d_s N_s$ and $d_n N_n$. Detailed balance requires that the ratio of the transmission probability from S to N and vice versa is $T_{s \rightarrow n} / T_{n \rightarrow s} = N_n / N_s$. This means that the transmission from the metal with the higher density of states is always less than 1.

In our numerical treatment of the SPE we studied the effect of a reduced transmission. Both transmissions, $T_{s \rightarrow n}$ and $T_{n \rightarrow s}$, were reduced by the factor $T < 1$. The result was that a reduction of the interface transmission did not alter the initial slope $|dT_c/dd_n|$, but it reduced the thickness range where one can observe the linear dependence of T_c on d_n . Since the role of the transmission T on the initial slope is important in the present investigation we have calculated and drawn in Fig. 1 the theoretical dependence of T_c on d_{Ag} for different transmissions of the interface. The numbers at the right side of the theoretical curves give the reduction factor T for the transmission through the interface into the Pb. The curves show that the initial slope remains constant. But with reduced transmission the transition temperature approaches a higher saturation value for T_c quicker. If one compares these theoretical curves of reduced transmission with the experimental curve one recognizes that the experimental curve

TABLE I. The experimental and theoretical slopes $d(T_s - T_c)^{-1}/d_{pb}$ are compared. The first five columns give the experimental code (containing the symbols of the normal conductor N and superconductor S), the thickness of N , the thermal coherence length ξ_T of N in the dirty limit, the transition temperature of N (if superconducting) and the ratio of the experimental density of states N_n/N_s (which includes electron-phonon enhancement). The sixth column gives the ratio between $m_{\text{exp}} = \left. \frac{d(T_s - T_c)^{-1}}{dd_{pb}} \right|_{\text{exp}}$ and $m_{\text{theo}} = \left. \frac{d(T_s - T_c)^{-1}}{dd_{pb}} \right|_{\text{theo}}$.

Exp.	d_n (nm)	ξ_T^l (nm)	T_n (K)	N_n/N_s	$m_{\text{theo}}/m_{\text{exp}}$
MgPbUW	3.08	9.1	0	0.572	4
AgPbJB	4.12	12.1	0	0.387	2.2
CuPbJE	3.29	10.8	0	0.603	2.5
AuPbJD	2.95	10.2	0	0.442	2.9
CdPbJJ	3.14	11.2	0.80	0.329	1.25
ZnPbUU	2.60	7.6	1.39	0.430	1.5
AlPbUT	2.15	9.6	2.28	0.833	1.7
InPbUP	3.21	13.6	4.1	0.663	1.2
SnPbUN	3.30	12.0	4.7	0.664	1.0

does not show the increased curvature of a reduced transmission.

C. The thin film regime

In Figs. 3–6 the experimental results for Ag/Pb, Mg/Pb, Zn/Pb, and Sn/Pb double layers are plotted. The big full circles show the inverse T_c reduction $(T_s - T_c)^{-1}$ as a function of the Pb thickness d_{pb} . The experimental points lie on straight lines with a finite intersection of the ordinate. The mean free path in the Pb film is about 3 nm and the resulting pair coherence length for the dirty limit is about 13 nm. (The coherence lengths of the metal N are collected in Table I.) In the same figures we have plotted the results of our numerical calculations as full up triangles. We observe two important results: (i) the theoretical points lie also on a straight line with the same ordinate intersection as the experimental results, (ii) for the double layers Ag/Pb, Mg/Pb, Zn/Pb there is a large discrepancy between the experimental and theoretical results. Only for the Sn/Pb double layer do we observe a good agreement between experiment and theory. For the other systems we have included an additional theoretical plot where we increased the density of states N_s of Pb artificially until the theoretical values agreed with the experiment. The experimental density of states of Pb is larger than its free electron density of states by almost a factor of 2. This is due to the strong electron-phonon mass enhancement $(1 + \lambda) \approx 2$, where $\lambda = 2 \int_0^\infty \alpha^2 F(\omega) d\omega / \omega$ is the electron-phonon parameter and $\alpha^2 F(\omega)$ is the Eliashberg function. For the Ag/Pb double layer we have to use an N_{pb} which is larger than the free electron density by a factor 4.3, while for Mg the factor was even 7.5. The resulting numerical results lie on the same straight line as the experimental points. (However, we do not give the strongly modified density of states any physical significance at this point.)

These results permit us to quantify the discrepancy between experiment and theory. As discussed in the Appendix the slopes $\left. \frac{d(T_s - T_c)^{-1}}{dd_{pb}} \right|_{\text{exp}}$ are closely related to the initial slope S_{sn} . But it is more transparent for demonstrating the discrepancy between experiment and theory to use the ratio of the experimental and theoretical slopes $m_{\text{exp}} = \left. \frac{d(T_s - T_c)^{-1}}{dd_{pb}} \right|_{\text{exp}}$ and $m_{\text{theo}} = \left. \frac{d(T_s - T_c)^{-1}}{dd_{pb}} \right|_{\text{theo}}$. The results for $m_{\text{exp}}/m_{\text{theo}}$ are collected in Table I.

The experimental results disagree dramatically with the theoretical predictions. It is also important to note that the experiments are performed in a regime where the theory is quite simple, essentially only averaging over the two metals S and N . It is surprising that this disagreement between experiment and theory has not been noticed in the past. The main reason is that the majority of the experimental and the theoretical work focused on NS double layers with thick normal metal films. Then superconductivity is only obtained for a finite thickness of the superconductor. In this case a comparison between experiment and theory requires many fit parameters such as the transmission of the interface and the mean free paths of the superconductor and the normal conductor. Therefore it is quite possible to fit the experimental data by using the wrong parameters that cannot be checked otherwise.

The physical origin of this disagreement between experiment and theory is not understood. Our theoretical simulation of the SPE uses the frame work of weak coupling superconductivity. Quench condensed Pb, In, and Sn are not weak coupling. The ratios of $2\Delta_0/(k_B T_s)$ for quench condensed films are 4.6 for Pb, 3.9 for In, and 4.0 for Sn [Refs. 38 and 39]. An obvious proposal would be to solve the superconducting proximity effect for strong coupling superconductors. This requires developing and solving a series of equations for the energy and position dependent gap function $\Delta(\mathbf{r}, \omega)$. This would be an extremely demanding job.

The normalized initial slope is proportional to the density of states ratio. Although the density of states can be modified in quench condensed films it is inconceivable that this explains a factor of 3 in the initial slope.

IV. CONCLUSION

In this paper, the superconducting proximity effect is investigated for SN double layers in a regime where the resulting T_c does not depend on the mean free path of the films and, within limits, not on the transmission of the interface. This includes the thin film regime and, in S/N double layers, the initial slope dT_c/dd_n at zero thickness d_n of the normal conductor.

For the superconducting layer S we always used Pb while the conductor N included a nonsuperconducting metal such as Cu, Ag, Au, and Mg and superconductors Cd, Zn, Al, In, and Sn with a T_c below the transition temperature of Pb. The experimental results for the transition temperature T_c are compared with a numerical calculation which was recently developed in our group. The results for the SN double layers can be divided into three groups:

When N represents a nonsuperconducting metal film ($N = \text{Cu, Ag, Au, and Mg}$) we observe grave deviations between experiment and theory by a factor of the order of 2.5.

When N represents a superconductor with a low T_c ($N = \text{Cd, Zn, Al}$) the disagreement between experiment and theory is reduced to a factor of about 1.5.

When N represents a superconductor with a T_c which is about half the T_c of Pb ($N = \text{In, Sn}$) then we observe a reasonably good agreement between experiment and theory.

Prior to our recent experiments we believed that the proximity effect between a superconductor and a normal conductor represented an intensively studied phenomenon with a good theoretical understanding. We are deeply puzzled by the large observed discrepancy between experiment and theory. The discrepancy is particularly disturbing since our experiments are performed in a regime where the theory is quite simple, essentially only averaging over the two metals S and N .

It would be very desirable if other theoretical approaches would give quantitative predictions for this thin film regime and the normalized initial slope in SN double layers. There have been a number of theoretical papers published which extended the proximity effect to more complex systems, for example between a superconductor and a ferromagnet but which include implicitly the simpler case of an SN double layer. These authors should be able to calculate quantitatively the normalized initial slope from their theory.

Experimentally it would be desirable to extend the measurements to SN layers where S is a weak coupling superconductor. This requires lower temperatures but permits the use of thicker films because the coherence lengths are larger at lower temperatures. Aluminum would be a good candidate for the superconductor if evaporated in ultrahigh vacuum so that the Al is not granular.

ACKNOWLEDGMENTS

The research was supported by the National Science Foundation Grant No. DMR-0439810.

APPENDIX: BACKGROUND OF THE NUMERICAL CALCULATION

The superconducting phase transition in zero magnetic field is generally of second order. The gap function $\Delta(\mathbf{r})$ is the order parameter of the phase transition. Therefore, close to the transition temperature T_c of the system, the gap function $\Delta(\mathbf{r})$ is small and only terms linear in the gap function contribute. This linear gap equation was first formulated by Gorkov.⁴⁰ Following de Gennes,^{36,8} Lueders,⁴¹ and one of the authors⁴² we use a different approach which leads to the following gap equation:³⁴

$$\Delta(\mathbf{r}) = V(\mathbf{r}) \int d^3\mathbf{r}' \int_{-\infty}^0 \frac{dt'}{\tau_T} \sum_{|\omega_n| < \Omega_D} e^{-2|\omega_n||t'|} \times \rho(v_F; \mathbf{r}, 0; \mathbf{r}', t') N(\mathbf{r}') \Delta(\mathbf{r}'). \quad (\text{A1})$$

Gorkov's original linear gap equation contains the product of two Green functions $G_{\omega_n}(\mathbf{r}, \mathbf{r}')$ and $G_{\omega_n}^*(\mathbf{r}, \mathbf{r}')$. The Green

function $G_{\omega_n}(\mathbf{r}, \mathbf{r}')$ represents the amplitude of an electron traveling from \mathbf{r}' to \mathbf{r} and the product $k_B T G_{\omega_n}(\mathbf{r}, \mathbf{r}') G_{\omega_n}^*(\mathbf{r}, \mathbf{r}')$ describes the pair amplitude of the Cooper pairs traveling from \mathbf{r}' to \mathbf{r} . Since the two single-particle Green functions are conjugate complex to each other, the product of their amplitudes is proportional to the probability of a single electron to travel from \mathbf{r}' to \mathbf{r} . Here we introduce the propagation density $\rho(v_F; \mathbf{r}, 0; \mathbf{r}', t')$ of an electron. If an electron starts at the time $t' < 0$ from the position \mathbf{r}' and propagates with Fermi velocity v_F into all directions then $\rho(v_F; \mathbf{r}, 0; \mathbf{r}', t')$ describes the probability density to find the electron at the time 0 at the position \mathbf{r} . The propagation of the pair amplitude is governed by the same "propagation density" $\rho(v_F; \mathbf{r}, 0; \mathbf{r}', t')$ as the propagation of single electrons.

During the travel time $|t'|$ from \mathbf{r}' to \mathbf{r} the pair amplitude decays because of a thermal loss of coherence between the two individual electron amplitudes. The subscript $\omega_n = (2n + 1)\pi k_B T / \hbar$ in $G_{\omega_n}(\mathbf{r}, \mathbf{r}') G_{\omega_n}^*(\mathbf{r}, \mathbf{r}')$ represents the Matsubara component of the pair amplitude. Each component decays as $\exp[-2|\omega_n|t']$ with time and arrives at $(\mathbf{r}, 0)$ with the magnitude $\exp(-2|\omega_n||t'|) / \tau_T^* N(\mathbf{r}) \rho(v_F; \mathbf{r}, 0; \mathbf{r}', t')$. As one recognizes the propagation in space and the decay in time can be separated. In superconductivity all (Matsubara) components up to the Debye frequency contribute.

Now the gap equation (A1) can be described in an "as if" or "ersatz" picture. Let us assume that we inject at the position \mathbf{r}' during the time interval $(t', t' + dt')$ in the past $N(\mathbf{r}') \Delta(\mathbf{r}') d^3\mathbf{r}' dt' / \tau_T$ electrons into volume element $d^3\mathbf{r}'$. These electrons will propagate from (\mathbf{r}', t') to an arbitrary position \mathbf{r} at the presence ($t=0$) according to the single electron propagation density $\rho(v_F; \mathbf{r}, 0; \mathbf{r}', t')$. Here [see Eq. (A1)] the arriving density of electrons, $\rho(v_F; \mathbf{r}, 0; \mathbf{r}', t') N(\mathbf{r}') \Delta(\mathbf{r}') d^3\mathbf{r}' dt' / \tau_T$, is multiplied with $e^{-2|\omega_n||t'|}$. Next we sum over all frequencies $|\omega_n| < \Omega_D$, perform the integral $\int d^3\mathbf{r}'$ over the whole volume of the system and the integral $\int_{-\infty}^0 dt'$ over time. Then we multiply the resulting density with the BCS interaction $V(\mathbf{r})$ at the position \mathbf{r} . The result has to recover the gap function $\Delta(\mathbf{r})$, for every position \mathbf{r} . The temperature at which the gap function is recovered self consistently is the transition temperature of the system.

The main numerical task is the calculation of the electron propagation density $\rho(v_F; \mathbf{r}, 0; \mathbf{r}', t')$. This is a problem which does not involve superconductivity. The superconductivity enters the problem only through the damping with the Matsubara frequencies, the BCS interaction and, of course, the self-consistency of the gap equation.

The Matsubara component with the smallest frequency for $n=0$ yields the decay rate $2\omega_0 = 2\pi k_B T / \hbar$. It decays as $\exp(-|t'| / \tau_T)$, where $\tau_T = \hbar / (2\pi k_B T)$ is the thermal coherence time.

1. Thin film limit

We turn to a double layer of two thin films S and N , which are both superconducting. This is shown in Fig. 7. We will evaluate the linear gap equation (A1) in the thin film limit.

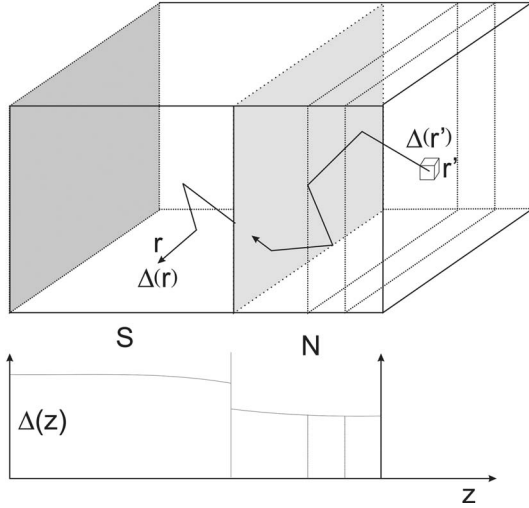


FIG. 7. The dynamics of the linear gap equation.

The thicknesses and density of states of the films are d_s , d_n and N_s , N_n . For normalization purposes the double layer may have an area A (in the x - y plane). In this geometry the gap function is only a function of the z direction. Therefore we take instead of the volume element $d^3\mathbf{r}'$ a sheet with the volume Adz' located between z' , $z'+dz'$. The sheet can be located in either N or S . For the discussion we choose N . The number of electrons which start during the time t' , $t'+dt'$ ($t' < 0$) from this sheet is $N_n\Delta_n(z')Adz'dt'/\tau_T$. If both films are in the thin film limit then after a very short time all these electrons are evenly distributed over both film. The equilibrium distribution in each film is proportional to the density of states. So their density has constant values in each film:

$$\rho_{n \rightarrow s} = \frac{N_s}{N_s d_s + N_n d_n} N_n \Delta_n(z') dz' dt' / \tau_T,$$

$$\rho_{n \rightarrow n} = \frac{N_n}{N_s d_s + N_n d_n} N_n \Delta_n(z') dz' dt' / \tau_T.$$

Here $\rho_{n \rightarrow s}$ is the density in S for electrons starting N . Similar density contributions are obtained from the electrons which start in S .

If the time it takes to achieve the equilibrium distribution is much shorter than τ_T then the densities are essentially constant for the whole dt' integration. The time integration yields $\sum_{|\omega_n| < \Omega_s} 1/(2|\omega_n|)$. Then the dz' integrations can be performed and one obtains for $\Delta_s(z)$

$$\Delta_s(z) = V_s \sum_{|\omega_n| < \Omega_s} \frac{1}{\tau_T} \frac{1}{2|\omega_n|} \left[\frac{N_s}{N_s d_s + N_n d_n} \left(N_s \int_{-d_s}^0 \Delta_s(z') dz' + N_n \int_0^{d_n} \Delta_n(z') dz' \right) \right].$$

This yields on the left side a constant value for $\Delta_s(z)$ which is given by the average of $\Delta_s(z')$ and $\Delta_n(z')$. Therefore consistency can only be achieved when both Δ_s and Δ_n are constant. This yields the solution for the thin film limit:

$$\Delta_s = V_s \sum_{|\omega_n| < \Omega_s} \frac{1}{\tau_T} \frac{1}{2|\omega_n|} \left[\frac{N_s}{N_s d_s + N_n d_n} (d_s N_s \Delta_s + d_n N_n \Delta_n) \right],$$

$$\Delta_n = V_n \sum_{|\omega_n| < \Omega_n} \frac{1}{\tau_T} \frac{1}{2|\omega_n|} \left[\frac{N_n}{N_s d_s + N_n d_n} (d_s N_s \Delta_s + d_n N_n \Delta_n) \right]. \quad (\text{A2})$$

These are exactly the two gap equations which deGennes derived for the thin film limit. We extended the equation to the case that the two metals have different Debye temperatures.

2. Structure of the numerical calculation

In the numerical solution of the dynamic linear gap equation (A1) the time integration is changed from $\int_{-\infty}^0 dt'$ to $\int_0^{\infty} dt'$. The propagation density $\rho(v_F; z, 0; z', t')$ depends only on the z coordinate. It is calculated semiclassically in a propagation simulation which covers the whole range from diffusive to ballistic propagation. Details can be found in Ref. 34.

The calculation is performed in a number of steps. (i) The superconductor is divided into Z_s layers of thickness λ_s , where $\lambda_s = d_s/Z_s$ (d_s is the thickness of the superconducting film). (ii) The BCS interaction V_s for the superconductor(s) is fitted, using the density of states N_s and the Debye temperature Θ_D . (iii) The time interval $\tau_d = 2\lambda_s/v_{F,s}$ is the time step of the numerical calculation ($v_{F,s}$ is the Fermi velocity of the superconductor). (iv) For the normal conductor (superconductor with lower T_c) the same time step is used by dividing its thickness in layers of thickness $\lambda_n = v_{F,n}\tau_d/2$. (v) An initial gap function $\Delta_v = \Delta(z_v)$ is introduced. Each cell is occupied at the time $t'=0$ with $O_v(0) = N(z_v)\lambda_v\Delta(z_v)$ electrons. [$N(z_v)$ is the local density of states, i.e., equal to N_s in the superconductor]. (vi) A procedure for diffusive and ballistic propagation of electrons in the different films is derived. (vii) The maximal transmission of an electron through the interface in each direction is calculated. It can be scaled down to include a barrier at the interface. (viii) The occupation $O_v(m)$ of the cell v is calculated in discrete steps for the time $t' = m\tau_d$. (ix) Due to thermal dephasing this density is, at each step, multiplied with the time factor $\sum_{\omega} e^{-2|\omega||t'|}$. (x) The sum over the time steps $\sum_m O_v(m) \sum_{\omega} e^{-2|\omega||t'|}$ is formed, multiplied with $(\tau_d/\tau_T)/\lambda_v$ and, in the superconductor(s), multiplied with V_s , the attractive electron-electron interaction. (xi) The resulting function $\tilde{\Delta}_v$ is the input Δ_v for the next iteration. (xii) Since the eigenvalue has to be 1 the ratio $r = \sum_v \tilde{\Delta}(z_v)/\sum_v \Delta(z_v)$ is calculated. If $r > 1$ ($r < 1$) one increases (lowers) the temperature. (xiii) The iteration process is completed when initial and final Δ_v agree with a relative accuracy of 10^{-5} . This is generally achieved after a few iterations. The details are described in Ref. 34.

3. Relation between normalized initial slope and the slope of the $1/(T_s - T_c)$ versus d_s plot

The slope $m = d(T_s - T_c)^{-1} / dd_s$ in the plots of $(T_s - T_c)^{-1}$ versus d_s is closely related to the normalized initial slope $S_{sn} = (T_s / d_s) |dT_c / dd_n|$. The thickness of the metals N in this series is very small, about 3 nm. Imagine that we condensed the same double layer in opposite sequence. Then the thin normal layer would reduce the transition temperature T_s of the superconductor S by $(T_s - T_c)$ and since d_n is so small we expect that the T_c reduction is still in the linear range. This means that

$$T_s - T_c \approx \left| \frac{dT_c}{dd_n} \right| d_n = S_{sn} T_s \frac{d_n}{d_s}$$

which yields

$$(T_s - T_c)^{-1} \approx \frac{1}{S_{sn} T_s d_n} d_s.$$

This suggests that a plot of $(T_s - T_c)^{-1}$ versus d_s should yield a straight line which goes through the origin with the slope $(S_{sn} T_s d_n)^{-1}$. In experiment and theory we observe indeed a straight line but it has a finite intersection with the ordinate. The reason is the following: When we reduce the thickness of the superconductor then d_n is no longer much smaller than d_s . In this case the resulting T_c no longer lies on the linear tangent of the T_c reduction but the dependence of T_c on d_n is already nonlinear. The smaller the thickness d_n is, the closer lies T_c to the tangent (at $d_n = 0$). For the parameters of our experiments the deviation (agreement) between S_{sn} and $1/(m T_s d_n)$ is about 10%. For the AgPbJB experiment (second row of Table I) we obtain from the experimental slope $d(T_s - T_c)^{-1} / dd_s$ the normalized initial slope of $S_{sn} = 0.67$. This is in good agreement with the results of Fig. 2.

-
- ¹H. Meissner, Phys. Rev. **117**, 672 (1960).
²P. Hilsch and R. Hilsch, Z. Phys. **167**, 511 (1962).
³P. Hilsch and R. Hilsch, Z. Phys. **180**, 10 (1964).
⁴P. G. DeGennes and E. Guyon, Phys. Lett. **3**, 168 (1963).
⁵J. J. Hauser, H. C. Theurer, and N. R. Werthamer, Phys. Rev. **136**, A637 (1964).
⁶G. Bergmann, Z. Phys. **187**, 395 (1965).
⁷G. v. Minnigerode, Z. Phys. **192**, 379 (1966).
⁸G. Deutscher and P. G. DeGennes, *Superconductivity*, edited by R. D. Parks (Marcel Dekker, New York, 1969), p. 1005.
⁹G. B. Arnold, Phys. Rev. B **18**, 1076 (1978).
¹⁰J. Bar-Sagi, Phys. Rev. B **18**, 3105 (1978).
¹¹V. Z. Kresin, Phys. Rev. B **25**, 157 (1982).
¹²M. Ashida, S. Aoyama, J. Hara, and K. Nagai, Phys. Rev. B **40**, 8673 (1989).
¹³M. Ashida, J. Hara, and K. Nagai, Phys. Rev. B **45**, 828 (1992).
¹⁴A. Z. Zaitsev, Physica C **185-189**, 2539 (1991).
¹⁵A. Z. Zaitsev, Physica B **203**, 274 (1997).
¹⁶A. Volkov, N. Allsopp, and C. J. Lambert, J. Phys.: Condens. Matter **8**, 45 (1996).
¹⁷R. G. Mints and I. B. Snapiro, Phys. Rev. B **57**, 10318 (1998).
¹⁸W. Belzig, F. K. K. Wilhelm, C. Bruder, G. Schoen, and A. D. Zaikin, Superlattices Microstruct. **25**, 1251 (1999).
¹⁹M. A. Sillanpää, T. T. Heikkilä, R. K. Lindell, and P. J. Hakonen, Europhys. Lett. **56**, 590 (2001).
²⁰M. Titov and H. Schomerus, Phys. Rev. B **67**, 024410 (2003).
²¹D. Huertas-Hernando and Y. V. Nazarov, Eur. Phys. J. B **44**, 373 (2005).
²²A. F. Volkov and A. V. Zaitsev, Phys. Rev. B **53**, 9267 (1996).
²³J. D. Lejeune and D. G. Naugle, J. Low Temp. Phys. **24**, 443 (1976).
²⁴S. Y. Hsu, J. M. Valles, P. W. Adams, and R. C. Dynes, Physica B **194**, 2337 (1994).
²⁵S. Gueron, H. Pothier, N. O. Birge, D. Esteve, and M. H. Devoret, Phys. Rev. Lett. **77**, 3025 (1996).
²⁶H. Courtois, P. Gandit, D. Mailly, and B. Pannetier, Phys. Rev. Lett. **76**, 130 (1996).
²⁷O. Bourgeois, A. Frydman, and R. C. Dynes, Phys. Rev. Lett. **88**, 186403 (2002).
²⁸M. Zhang and G. Bergmann, Europhys. Lett. **69**, 442 (2005).
²⁹D. Garrett, M. Zhang, and G. Bergmann, Eur. Phys. J. B **39**, 199 (2004).
³⁰T. Kouh and J. M. Valles, Phys. Rev. B **67**, 140506(R) (2003).
³¹R. Banerjee, P. Vasa, G. Thompson, and P. Ayyub, Solid State Commun. **127**, 349 (2003).
³²O. Bourgeois, A. Frydman, and R. C. Dynes, Phys. Rev. B **68**, 092509 (2003).
³³L. Covaci and F. Marsiglio, Phys. Rev. B **73**, 014503 (2006).
³⁴G. Bergmann, Phys. Rev. B **72**, 134505 (2005).
³⁵N. R. Werthamer, Phys. Rev. **132**, 2440 (1963).
³⁶P. G. DeGennes, Rev. Mod. Phys. **36**, 225 (1964).
³⁷C. Kittel, *Introduction to Solid State Physics*, 7th ed. (John Wiley and Sons, New York, 1996).
³⁸G. Bergmann, Z. Phys. **228**, 25 (1969).
³⁹G. Zimba and G. Bergmann, Z. Phys. **237**, 410 (1970).
⁴⁰L. P. Gorkov, Pis'ma Zh. Eksp. Teor. Fiz. **37**, 1407 (1959); JETP **10**, 998 (1960).
⁴¹G. Lueders and K. D. Usadel, in *Springer Tracts in Modern Physics*, edited by G. Hoehler, (Springer Verlag, Berlin, 1971), Vol. 56, p. 1.
⁴²G. Bergmann, Z. Phys. **234**, 70 (1970).
⁴³L. Cooper, Phys. Rev. Lett. **6**, 689 (1961).